Am J Physiol Renal Physiol 309: F474–F483, 2015.
First published June 24, 2015; doi:10.1152/ajprenal.00477.2014.

TRANSLATIONAL PHYSIOLOGY

Cyclophosphamide-induced vasopressin-independent activation of aquaporin-2 in the rat kidney

Sua Kim,[1] Hyo-Jung Choi,[2] Chor Ho Jo,[1] Joon-Sung Park,[3] Tae-Hwan Kwon,[2] and Gheun-Ho Kim[1,3]

[1]*Institute of Biomedical Sciences, Hanyang University College of Medicine, Seoul, Korea;* [2]*Department of Biochemistry and Cell Biology, Kyungpook National University School of Medicine, Taegu, Korea; and* [3]*Division of Nephrology, Department of Internal Medicine, Hanyang University College of Medicine, Seoul, Korea*

Submitted 22 August 2014; accepted in final form 16 June 2015

Kim S, Choi HJ, Jo CH, Park JS, Kwon TH, Kim GH. Cyclophosphamide-induced vasopressin-independent activation of aquaporin-2 in the rat kidney. *Am J Physiol Renal Physiol* 309: F474–F483, 2015. First published June 24, 2015; doi:10.1152/ajprenal.00477.2014.—Because cyclophosphamide-induced hyponatremia was reported to occur without changes in plasma vasopressin in a patient with central diabetes insipidus, we hypothesized that cyclophosphamide or its active metabolite, 4-hydroperoxycyclophosphamide (4-HC), may directly dysregulate the expression of water channels or sodium transporters in the kidney. To investigate whether intrarenal mechanisms for urinary concentration are activated in vivo and in vitro by treatment with cyclophosphamide and 4-HC, respectively, we used water-loaded male Sprague-Dawley rats, primary cultured inner medullary collecting duct (IMCD) cells, and IMCD suspensions prepared from male Sprague-Dawley rats. In cyclophosphamide-treated rats, significant increases in renal expression of aquaporin-2 (AQP2) and Na-K-2Cl cotransporter type 2 (NKCC2) were shown by immunoblot analysis and immunohistochemistry. Apical translocation of AQP2 was also demonstrated by quantitative immunocytochemistry. In both rat kidney and primary cultured IMCD cells, significant increases in AQP2 and vasopressin receptor type 2 (V2R) mRNA expression were demonstrated by real-time quantitative PCR analysis. Confocal laser-scanning microscopy revealed that apical translocation of AQP2 was remarkably increased when primary cultured IMCD cells were treated with 4-HC in the absence of vasopressin stimulation. Moreover, AQP2 upregulation and cAMP accumulation in response to 4-HC were significantly reduced by tolvaptan cotreatment in primary cultured IMCD cells and IMCD suspensions, respectively. We demonstrated that, in the rat kidney, cyclophosphamide may activate V2R and induce upregulation of AQP2 in the absence of vasopressin stimulation, suggesting the possibility of drug-induced nephrogenic syndrome of inappropriate antidiuresis (NSIAD).

cyclophosphamide; aquaporin-2; Na-K-2Cl cotransporter type 2; vasopressin receptor type 2; hyponatremia

CYCLOPHOSPHAMIDE IS AN ALKYLATING agent used extensively to treat malignancy and rheumatological disease. It can produce an antidiuretic effect when a high dose is injected intravenously into water-loaded patients (35). We recently reported that the occurrence of hyponatremia was not rare when low-dose pulse cyclophosphamide was given to patients with lupus nephritis and lymphoma (23). However, the mechanisms by which cyclophosphamide induces water retention in the kidney have not been defined.

Although many drugs can cause water retention, mechanistic explanations as to how they decrease water excretion from the kidneys are lacking. In contrast to drugs that enhance vasopressin release, such as vincristine, cyclophosphamide is classified as a drug that potentiates the renal action of vasopressin (34). More specifically, water retention may result from the direct effects of cyclophosphamide on the collecting duct epithelium, because plasma vasopressin levels are not elevated in patients following the administration of intravenous cyclophosphamide (2, 5, 22). Furthermore, antidiuresis was reported to occur in response to intravenous cyclophosphamide in an 8-yr-old girl with central diabetes insipidus (6), excluding the possibility of the syndrome of inappropriate antidiuretic hormone secretion (SIADH).

These previous studies led us to hypothesize that cyclophosphamide or its active metabolites may directly dysregulate the expression of water channels and/or sodium transporters in the kidney. According to DeFronzo et al. (13), the effect of cyclophosphamide-induced water retention was related temporally with the urinary excretion of active metabolites of the drug, and 4-hydroperoxycyclophosphamide (4-HC) is the main hepatic active metabolite of cyclophosphamide (36).

This study was undertaken to investigate whether intrarenal mechanisms of urinary concentration are activated by treatment with cyclophosphamide or 4-HC. In particular, we explored the roles of the V2 vasopressin receptor (V2R), aquaporin-2 water channel (AQP2), and Na-K-2Cl cotransporter type 2 (NKCC2) in cyclophosphamide-induced water retention.

MATERIALS AND METHODS

Animal experiments. Specific pathogen-free male Sprague-Dawley rats weighing 210–230 g (Orient Bio, Seongnam, Korea) were used. Based on the results of our preliminary study (20), we performed two different animal experiments. In each experiment, the rats were randomly divided into vehicle-treated controls and cyclophosphamide-treated rats. In animal *experiment 1*, kidneys were harvested 12 h after a single intraperitoneal administration of cyclophosphamide [25 mg/kg body wt (BW)], whereas in animal *experiment 2*, kidneys were harvested 72 h after a single intraperitoneal administration of cyclophosphamide (50 mg/kg BW) (Fig. 1). Before cyclophosphamide administration, rats were water-loaded with a gelled-agar diet for 3 days. The diet comprised 1% agar, 72% water, and 27% powdered rat chow (15), and the rats received 70 g of this preparation per 200 g BW each day. Plasma and urine were obtained at the end of

Address for reprint requests and other correspondence: G.-H. Kim, Dept. of Internal Medicine, Hanyang Univ. College of Medicine, 222-1 Wangsimni-ro Seongdong-gu, Seoul 133-792, South Korea (e-mail: kimgh@hanyang.ac.kr).

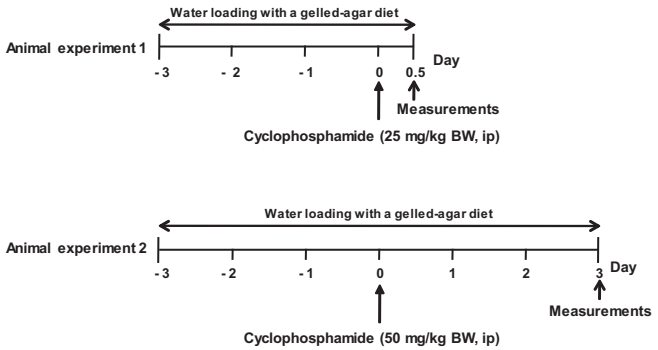

Fig. 1. Study design of animal experiments. Rats were water loaded with a gelled-agar diet for 3 days before cyclophosphamide administration. In animal *experiment 1*, kidneys were harvested 12 h after a single intraperitoneal administration of cyclophosphamide [25 mg/kg body wt (BW)]. In animal *experiment 2*, kidneys were harvested 3 days after a single intraperitoneal administration of cyclophosphamide (50 mg/kg BW). The gelled-agar diet was provided throughout the study period.

each animal experiment, and vasopressin levels were determined from EDTA plasma by RIA (Vasopressin Direct RIA, Buhlmann Laboratories). This experimental protocol was approved by the Institutional Animal Care and Use Committee of Hanyang University.

Immunoblot analysis. Rat kidneys were homogenized and prepared for semiquantitative immunoblotting according to our previous protocols (29, 30). Protein samples were separated by SDS-PAGE, using 8% gels for NKCC2 protein expression and 12% gels for aquaporin-1 water channel (AQP1), AQP2, AQP3, AQP7, and GAPDH. Proteins were transferred electrophoretically from unstained gels to nitrocellulose membranes (Bio-Rad, Hercules, CA). After blocking with 5% skim milk in PBS-T (80 mM Na_2HPO_4, 20 mM NaH_2PO_4, 100 mM NaCl, 0.1% Tween 20, pH 7.5) for 1 h, membranes were probed overnight at 4°C with the respective primary antibodies: rabbit polyclonal anti-AQP1, anti-AQP2, anti-AQP3, and anti-AQP7 (Alomone Labs, Jerusalem, Israel), rabbit polyclonal anti-NKCC2 (kindly donated by Dr. Mark Knepper at the National Institutes of Health, Bethesda, MD), or rabbit polyclonal anti-GAPDH (Cell Signaling Technology, Beverly, MA). The secondary antibody was goat anti-rabbit IgG conjugated to horseradish peroxidase (Jackson ImmunoResearch, West Grove, PA). The sites of antibody-antigen reaction were viewed using enhanced chemiluminescence (GenDEPOT, Barker, TX), and the band densities on immunoblots were quantified by densitometry using a laser scanner and Quantity One software (Basic version 4.6.9, Bio-Rad).

Immunohistochemical staining of rat kidneys. Kidneys were perfused by retrograde perfusion via the abdominal aorta with 1% PBS to remove blood and then with periodate-lysine-paraformaldehyde (PLP; 0.01 M $NaIO_4$, 0.075 M lysine, 2% paraformaldehyde, in 0.0375 M Na_2HPO_4 buffer, pH 6.2) for 10 min for kidney fixation. After completion of perfusion, each kidney was sliced into 4-mm-thick pieces and immersed in 2% PLP solution overnight at 4°C. Renal tissues were fixed in 10% neutral-buffered formalin and embedded in paraffin. Embedded kidney slices were sectioned to 4 μm in thickness on a microtome. Sections were deparaffinized with a graded series of ethanol and treated with 3% H_2O_2 for 30 min to eliminate endogenous peroxidase activity. Heat-induced epitope retrieval was performed using a citrate buffer (pH 6.0), and sections were blocked with 10% normal donkey serum for 1 h. They were then incubated overnight at 4°C with their respective primary antibodies. Sections were then washed in PBS and incubated for 2 h with a Dako Envision kit (Dako, Glostrup, Denmark) at room temperature. They were washed with Tris buffer and incubated in 0.05% 3,3′-diaminobenzidine (DAB) and 0.033% H_2O_2. Tissues were counterstained with hematoxylin, and slides were mounted with Canadian balsam (Sigma, St. Louis, MO).

Quantification of AQP2 immunofluorescence in rat kidneys for subcellular localization. Rat kidney sections prepared as above were incubated overnight at 4°C with anti-AQP2 polyclonal antibody, rinsed in PBS, and then incubated with FITC-conjugated secondary antibody (Jackson ImmunoResearch Laboratories) for 1 h at room temperature. Quantification of mean fluorescence intensity (MFI) of apical vs. cytoplasmic AQP2 immunostaining in rat kidneys was performed from raw images (17, 31). Sections from three vehicle-treated control rats and three 12-h cyclophosphamide-treated rats were immunostained concurrently under identical conditions. All digital images were acquired using identical exposure parameters under a Leica confocal microscope (TCS SP5, Leica Microsystems, Wetzlar, Germany). Regions corresponding to AQP2-associated fluorescence in the apical membrane and cytoplasm of the collecting duct cells were selected and analyzed with LAS X software (version 1.0.0, Leica Microsystems). The fluorescent signal was obtained at every 0.1 μm in the horizontal directions. The MFI of cortex and medulla was measured, and all MFIs were corrected for a background value determined for each image taken by measuring the pixel intensity in several locations of the darkest cells and selecting the lowest value. The MFI ratio of the apical-to-cytoplasmic region was calculated. The average ratio from 10 to 20 tubular cells was used for each animal.

Primary culture of rat kidney inner medullary collecting duct cells. Primary cultures enriched in inner medullary collecting duct (IMCD) cells were prepared from pathogen-free male Sprague-Dawley rats (200–250 g, Orient Bio), as described previously (9, 24). Briefly, rats were anesthetized under enflurane inhalation, and kidneys were rapidly removed. After isolating an IMCD cell suspension, cells were seeded on semipermeable filters of a Transwell system (0.4-μm pore size, Transwell Permeable Supports, catalog no. 3460, Corning). IMCD cells were fed every 48 h and were grown in hypertonic culture medium (640 mosmol/kgH_2O) supplemented with 10% fetal bovine serum at 37°C in a 5% CO_2-95% air atmosphere for 3 days, and then in fetal bovine serum-free culture medium for an additional day before

Table 1. *Primer sequences for qPCR*

Gene	Forward (F) and reverse (R) Primer Sequences	PCR Product, bp	GenBank Accession No.
AQP1	F 5′-CTGCTGGCCATTGACTACACTG-3′ R 5′-GGTTTGAGAAGTTGCGGGTGAG-3′	89	NM_012778.1
AQP2	F 5′-GCTCTTCATCTTTGCTCAGCGT-3′ R 5′-CCCCACGGATTTCTACTGGAGT-3′	125	NM_012909.2
AQP3	F 5′-AGCAGATCTGAGTGGGCAGT-3′ R 5′-CTTGGGCTTAAGAGGGGAAC-3′	214	NM_031703.1
NKCC2	F 5′-CGGGTCGTCTAGATCCAAAA-3′ R 5′-ATGGACTTGGAAACGACTGG-3′	189	NM_001270617
V2R	F 5′-GCTCTTCATCTTTGCTCAGCGT-3′ R 5′-TCCAGGTGACATAGGCACGAA-3′	110	NM_019136

qPCR, quantitative PCR; AQP1, aquaporin-1 water channel; AQP2, aquaporin-2 water channel; AQP3, aquaporin-3 water channel; AQP7, aquaporin-7 water channel; NKCC2, Na-K-2Cl cotransporter type 2; V2R, V2 vasopressin receptor.

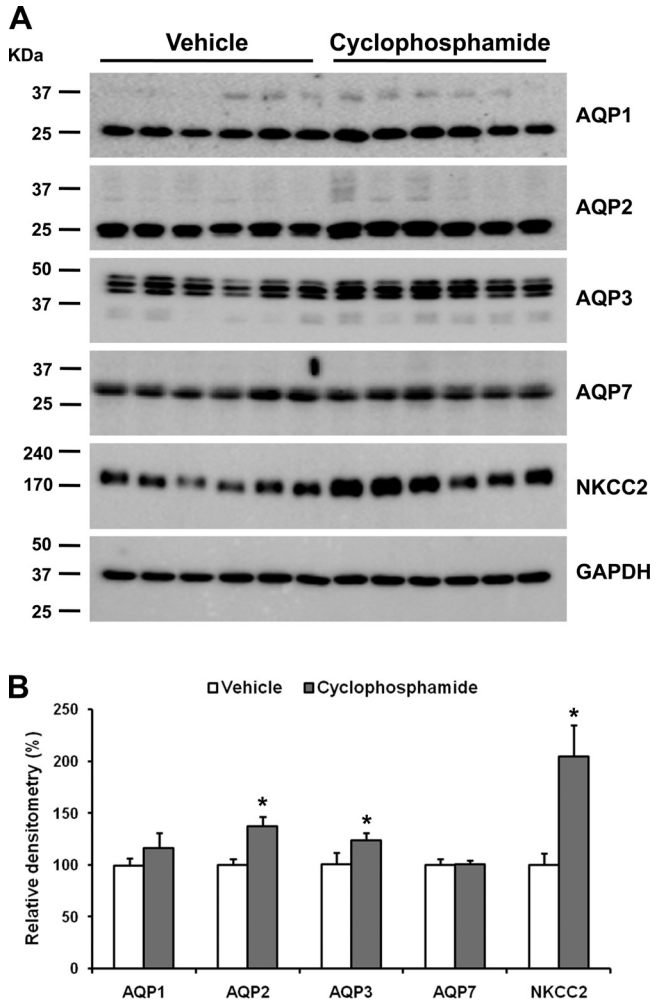

Fig. 2. *A*: immunoblots of aquaporin-1 (AQP1), aquaporin-2 (AQP2), aquaporin-3 (AQP3), and Na-K-2Cl cotransporter type 2 (NKCC2) in rat kidneys from animal *experiment 1*. Kidneys were harvested 12 h after a single intraperitoneal administration of cyclophosphamide (25 mg/kg BW) in Sprague-Dawley rats. The immunoblots were reacted with anti-AQP1 (~28-kDa nonglycosylated and ~35-kDa glycosylated bands), anti-AQP2 (~29-kDa nonglycosylated and ~35-kDa glycosylated bands), anti-AQP3 (~27-kDa nonglycosylated and ~40-kDa glycosylated bands), anti-AQP7 (~28 kDa), anti-NKCC2 (~170 kDa), and anti-GAPDH antibody (~37 kDa). Each lane was loaded with a protein sample from a different rat. *B*: densitometric analyses revealed significant increases in AQP2, AQP3, and NKCC2 in cyclophosphamide-treated rats vs. control rats. $*P < 0.05$.

the experiment at *day 5*. Culture medium was Dulbecco's modified Eagle's medium/F12 without phenol red, containing 80 mM urea, 130 mM NaCl, 10 mM HEPES, 2 mM L-glutamine, 10,000 U/ml penicillin/streptomycin, 50 nM hydrocortisone, 5 pM 3,3,5-triiodo-thyronine, 1 nM sodium selenate, 5 mg/l transferrin, and 10% fetal bovine serum (pH 7.4, 640 mosmol/kgH_2O). Previously, V2R-mediated small interfering (si)RNA delivery against AQP2 was demonstrated in these cells (18).

To study whether 4-HC treatment induces AQP2 upregulation, IMCD cells were treated for 24 h with vehicle (FBS-free culture medium) or two different doses of 4-HC at both the apical and basolateral sides of the cells. 4-HC was purchased from Niomec (Bielefeld, Germany), and therapeutic (10 μM) or toxic (30 μM) concentrations of 4-HC were chosen based on clinical (1, 8) and preclinical (3, 7) study findings. Next, to examine whether 4-HC-induced AQP2 upregulation was mediated by V2R stimulation, primary cultured IMCD cells were pretreated with a V2R antagonist, tolvaptan (10 or 50 nM, basolateral side only), for 3 h, followed by cotreatment with dDAVP (1 nM, basolateral side only) or 4-HC (10 μM, basolateral side only) for an additional 24 h. For semiquantitative immunoblotting, cell lysate was obtained in RIPA buffer (10 mM Tris·HCl, 0.15 M NaCl, 1% NP-40, 1% Na-deoxycholate, 0.5% SDS, 0.02% sodium azide, 1 mM EDTA, pH 7.4) containing proteinase and phosphatase inhibitors (0.4 μg/ml leupeptin, 0.1 mg/ml pefabloc, 1 mM Na_3VO_4, 25 mM NaF, and 0.1 μM okadoic acid). For immunocytochemistry, cells were fixed with 3% paraformaldehyde in PBS, pH 7.4, for 20 min at room temperature.

Immunofluorescence microscopy of primary cultured IMCD cells. IMCD cells were grown to confluence in a Transwell chamber (0.4-μm pore size, Transwell Permeable Supports, catalog no. 3460, Corning) for 4 days and treated on *day 5* after seeding according to the experimental protocols (9, 23). On *day 5*, IMCD cells were subjected to treatment with vehicle or 4-HC (10 or 30 μM, both apical and basolateral sides of the cells) for 1 day and then fixed with 3% paraformaldehyde in PBS, pH 7.4, for 20 min at room temperature. After fixation, cells were washed twice in PBS and permeabilized with 0.3% Triton X-100 in PBS at room temperature for 15 min. Cells were washed and incubated with anti-AQP2 antibody (1:400, AB3274, Millipore) in PBS overnight at 4°C, and nuclei were stained with 4,6-diamidino-2-phenylindole (DAPI; D1306, Molecular Probes). After incubation, cells were washed in PBS and incubated with goat-anti-rabbit IgG Alexa Fluor 488 secondary antibody (A11008, Molecular Probes) for 2 h at room temperature. Cells were washed in a

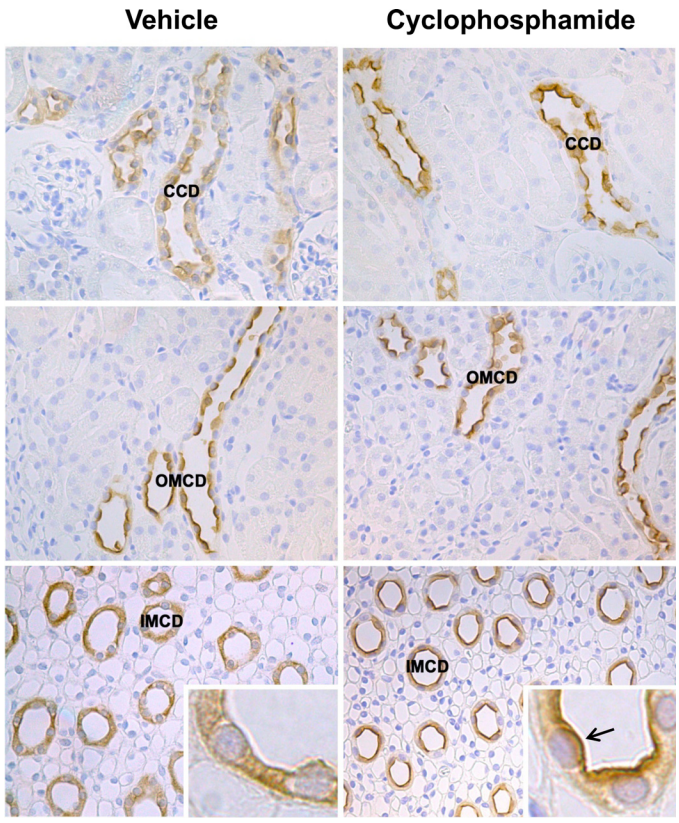

Fig. 3. Immunohistochemistry for AQP2 in rat kidneys from animal *experiment 1*. Kidneys were harvested 12 h after a single intraperitoneal administration of cyclophosphamide (25 mg/kg BW) in Sprague-Dawley rats. In cyclophosphamide-treated rats, immunostaining for AQP2 appears to be increased along the collecting duct. The arrow in the *inset* (high magnification) of the inner medullary collecting duct (IMCD) indicates that apical AQP2 labeling was remarkably enhanced by cyclophosphamide administration. CCD, cortical collecting duct; OMCD, outer medullary collecting duct.

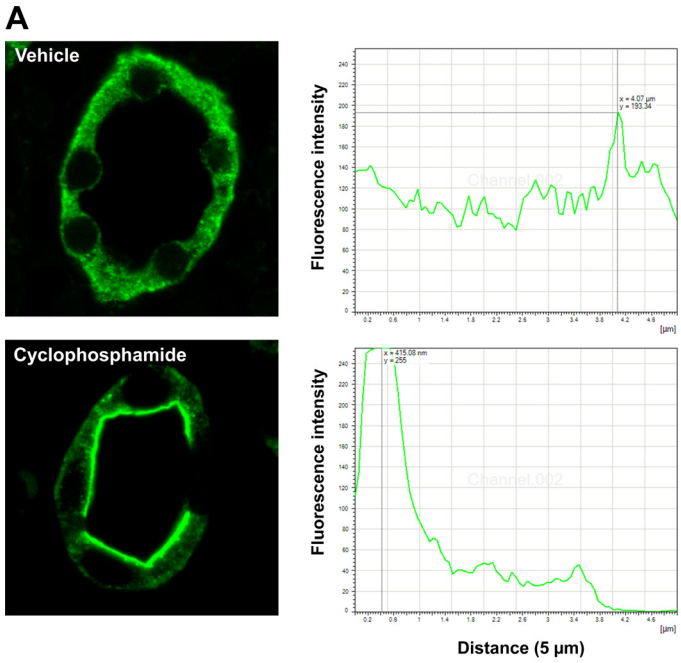

Fig. 4. *A*: AQP2 immunofluorescence for subcellular localization in rat kidneys from animal *experiment 1*. Representative confocal microscopy images of inner medulla are shown from a vehicle-treated and a cyclophosphamide-treated rat. *B*: bar graphs compare the mean fluorescence intensity (MFI) ratios between the apical and cytoplasmic regions in cortex and medulla. $*P < 0.05$.

hydrophilic mounting medium containing antifading reagent (P36930, Molecular Probes). AQP2 immunolocalization was observed using a laser-scanning confocal microscope (Zeiss LSM 5 EXCITER, Jena, Germany).

The immunofluorescence of AQP2 was detected at 530 nm with an excitation wavelength of 490 nm. During evaluating of 4-HC-induced subcellular redistribution of AQP2, identical microscope settings (light intensity, gain value, sampling period, and averaging) were used between groups, and the observer was blinded to treatment data. Digital images were collected and analyzed using the Zeiss Aim Image Examiner program. *X-Z* images of AQP2-labeled cells were randomly selected from each group, and immunofluorescence intensity per distance (60 pixels) from the apical pole to the base of the cells (vertical lines drawn just next to the nuclei stained with DAPI) was acquired. The total number of cells examined was 150 (50 for vehicle-treated controls, 50 for the 10 μM 4-HC-treated group, and 50 for the 30 μM 4-HC-treated group).

Quantitative PCR analysis. Total RNA was isolated from rat kidneys and primary cultured IMCD cells with TRIzol Reagent (Life Technologies, Carlsbad, CA). RNA was quantified by spectrophotometry, and cDNA synthesis was performed on 3 μg of RNA with SuperScript III Reverse Transcriptase (Life Technologies). For quantitative (q) PCR, 100 ng of cDNA served as a template for PCR amplification using the Brilliant SYBR green QPCR master mix, according to the manufacturer's instructions (FastStart DNA Master SYBR Green I; Roche Molecular Biochemicals, Mannheim, Germany). A serial dilution (1 ng-fg/μl) of cDNA was used as a template to generate a standard curve. Nested primers were used to amplify the standard and kidney cDNA samples (Table 1). Standard and unknown samples were amplified in duplicate in 96-well plates. The thermal profile of the LightCycler Instrument (Roche Molecular Biochemicals) was optimized as follows: an initial denaturation for 5 min at 95°C followed by 45 amplification cycles, each consisting of 10 s at 95°C and 45 s at 60°C. Specificity was verified by melting-curve analysis. Relative mRNA expression was determined by normalizing the expression of each target to GAPDH mRNA levels. Results were analyzed by the $2^{-\Delta\Delta Ct}$ method (25).

cAMP measurement in IMCD suspensions. Intracellular cAMP levels were measured in IMCD suspensions prepared from normal kidneys of Sprague-Dawley rats (200–250 g, Orient Bio), as previously described (10, 14). Acutely isolated IMCD suspensions were incubated with 1 mM IBMX for 30 min to inhibit cyclic nucleotide phosphodiesterases. In the presence of IBMX, 10 nM dDAVP, 10 μM 4-HC, and 10 μM 4-HC+100 nM tolvaptan (S2593, Selleckchem) suspensions were treated for an additional 30 min. The reaction was terminated by adding 10% trichloroacetic acid and placing the sample tube on ice for 10 min. The cAMP levels in the supernatant were determined using a competitive enzyme immunoassay kit (Cayman Chemical, Ann Arbor, Ml). The protein content of each suspension aliquot was measured, and the results were expressed in picomoles per milligram protein.

Statistics. Values are presented as means ± SE. Quantitative comparisons between groups were performed using the Mann-Whitney *U*-test (Statview software; Abacus Concepts, Berkeley, CA). To

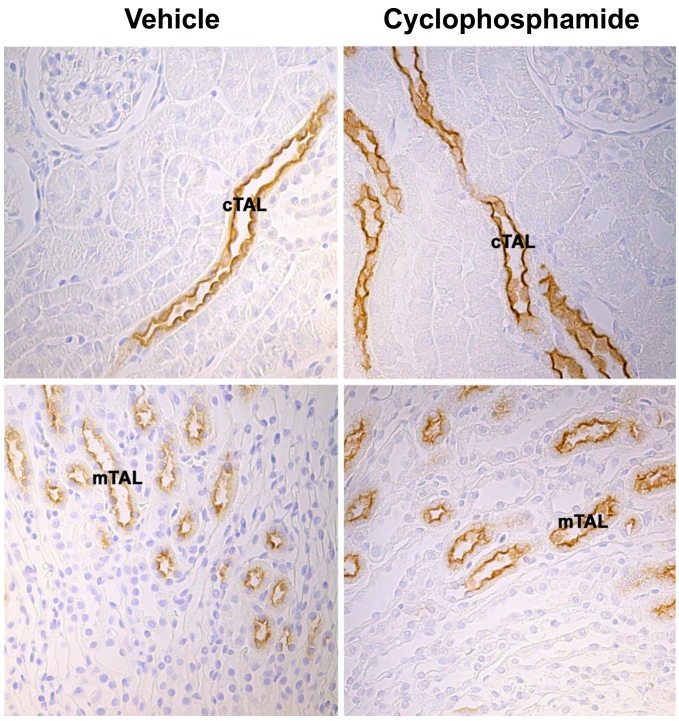

Fig. 5. Immunohistochemistry for NKCC2 in rat kidneys from animal *experiment 1*. Kidneys were harvested 12 h after a single intraperitoneal administration of cyclophosphamide (25 mg/kg BW) in Sprague-Dawley rats. In cyclophosphamide-treated rats, immunostaining for NKCC2 appears to be increased in the thick ascending limb. cTAL, cortical thick ascending limb; mTAL, medullary thick ascending limb.

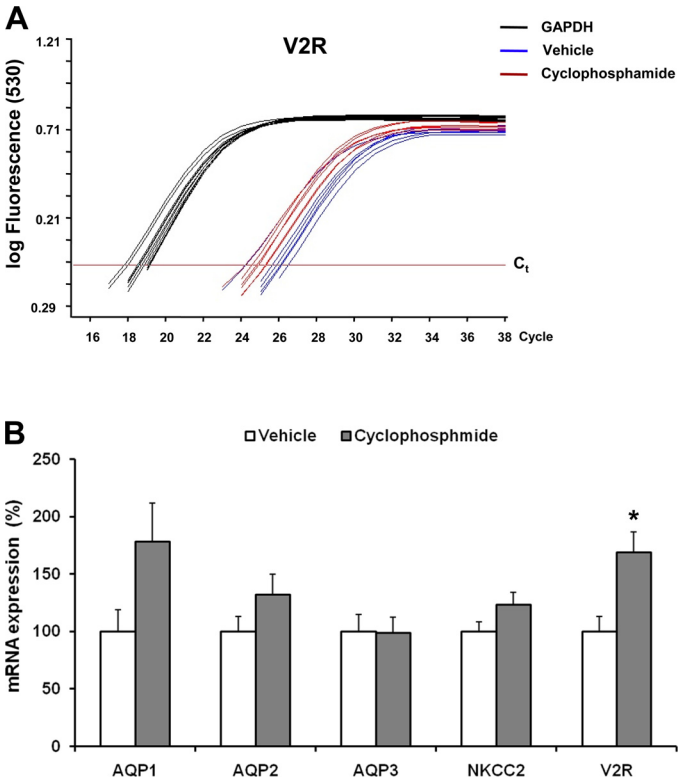

Fig. 6. Real-time quantitative PCR for AQP1, AQP2, AQP3, NKCC2, and vasopressin-2 receptor (V2R) in rat kidneys from animal *experiment 1*. Kidneys were harvested 12 h after a single intraperitoneal administration of cyclophosphamide (25 mg/kg BW) in Sprague-Dawley rats. *A*: V2R graphs of fluorescence against cycle number were discriminated between vehicle-treated controls (blue) and cyclophosphamide-treated rats (red). *B*: the level of V2R mRNA expression was significantly increased by cyclophosphamide administration vs. vehicle administration. Horizontal bar represents the threshold cycle (C_t). *$P < 0.05$.

facilitate immunoblot and qPCR comparisons, we normalized the band density or the relative mRNA values by dividing them by the mean value for the vehicle-treated control group. Thus the mean for the control group was defined as 100%. $P < 0.05$ was considered to indicate statistical significance.

RESULTS

Renal response to cyclophosphamide administration in Sprague-Dawley rats. In animal *experiment 1*, kidneys were harvested 12 h after a single administration of cyclophosphamide (25 mg/kg BW) (Fig. 1). Urine output measured over the experimental period decreased significantly in cyclophosphamide-administered rats ($n = 6$, 15.3 ± 1.8 ml) compared with vehicle-treated controls ($n = 6$, 22.5 ± 2.4 ml; $P < 0.05$). However, neither urine osmolality (824 ± 73 vs. 763 ± 58 mosmol/kgH_2O) nor plasma sodium concentration (143 ± 2 *vs.* 143 ± 1 mmol/l) differed significantly between groups.

In the kidney, expression of AQP2, NKCC2, and V2R was upregulated by cyclophosphamide administration. Immunoblotting results for AQP1, AQP2, AQP3, AQP7, and NKCC2 from whole kidney homogenates and densitometric values are shown in Fig. 2. Whereas alterations in levels of AQP1 and AQP7 were not significant, expression of AQP2 (137 ± 10 vs. 100 ± 6%; $P = 0.01$), AQP3 (123 ± 7 vs. 100 ± 10%; $P < 0.05$), and NKCC2 (205 ± 32 vs. 100 ± 11%; $P < 0.05$) was significantly increased by cyclophosphamide administration. These immunoblot findings were confirmed by immunohistochemistry. Figure 3 shows that cyclophosphamide-treated rats had stronger apical AQP2 labeling along the collecting duct than controls. This change in AQP2 subcellular localization was quantitatively evaluated based on immunofluorescence intensity using confocal laser-scanning microscopy. Figure 4 demonstrates that cyclophosphamide treatment induced remarkable increases in apical-to-cytoplasmic MPI ratios for AQP2 immunofluorescence labeling in the cortex (6.21 ± 0.83 vs. 1.69 ± 0.26; $P < 0.05$) and medulla (7.90 ± 0.40 vs. 2.80 ± 0.50; $P < 0.05$).

In Fig. 5, NKCC2 immunostaining in the thick ascending limb appears to be increased in cyclophosphamide-treated rat kidneys compared with controls. When mRNA expression levels were examined by qPCR, a significant increase in V2R

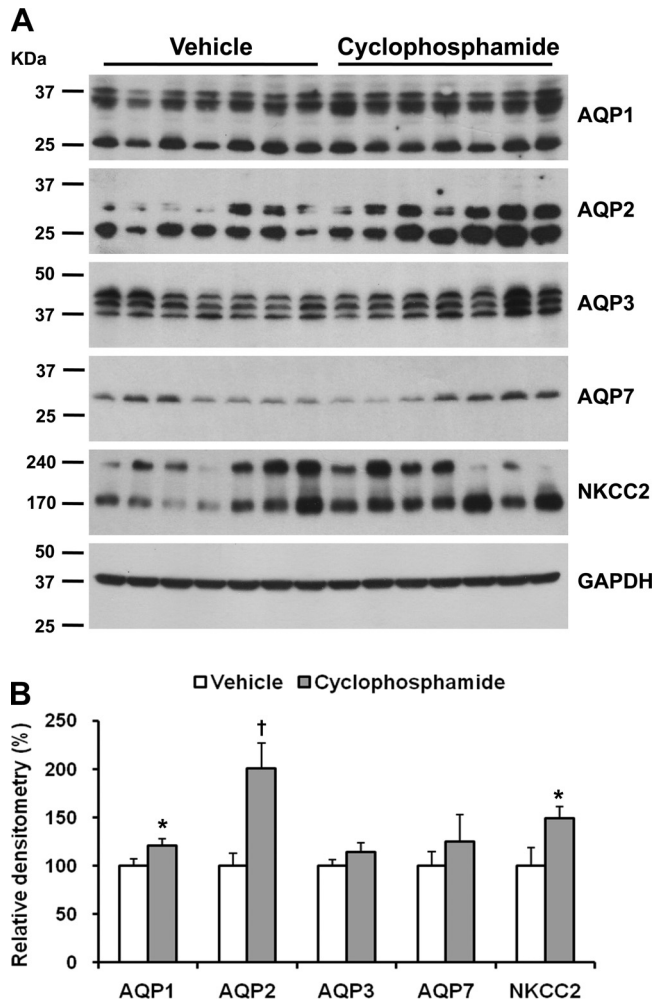

Fig. 7. *A*: immunoblots of AQP1, AQP2, AQP3, and NKCC2 in rat kidneys from animal *experiment 2*. Kidneys were harvested 72 h after a single intraperitoneal administration of cyclophosphamide (50 mg/kg BW) in Sprague-Dawley rats. The immunoblots were reacted with anti-AQP1 (~28-kDa nonglycosylated and ~35-kDa glycosylated bands), anti-AQP2 (~29-kDa nonglycosylated and ~35-kDa glycosylated bands), anti-AQP3 (~27-kDa nonglycosylated and ~40-kDa glycosylated bands), anti-AQP7 (~28 kDa), anti-NKCC2 (~170 kDa), and anti-GAPDH antibody (~37 kDa). Each lane was loaded with a protein sample from a different rat. *B*: densitometric analyses revealed significant increases in AQP1, AQP2, and NKCC2 expression in cyclophosphamide-treated rats vs. control rats. *$P < 0.05$. †$P < 0.01$.

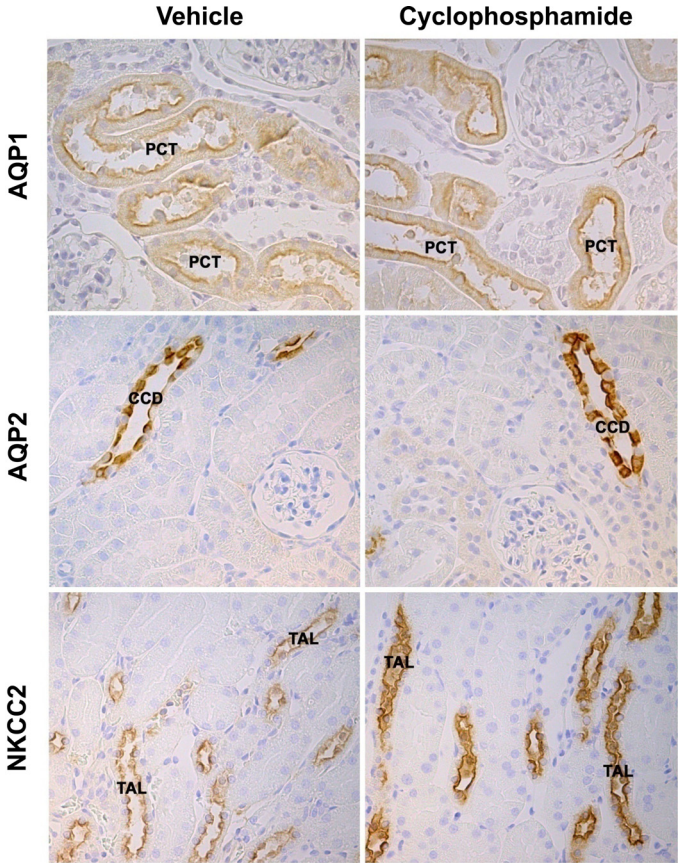

Fig. 8. Immunohistochemistry for AQP1, AQP2, and NKCC2 in rat kidneys from animal *experiment 2*. Kidneys were harvested 72 h after a single intraperitoneal administration of cyclophosphamide (50 mg/kg BW) in Sprague-Dawley rats. In cyclophosphamide-treated rats, immunostaining for AQP1, AQP2, and NKCC2 appears to be increased in the proximal convoluted tubule (PCT), cortical collecting duct (CCD), and thick ascending limb (TAL) compared with control rats.

was observed in cyclophosphamide-treated rats compared with controls (169 ± 18 vs. 100 ± 13%; $P < 0.05$). Although AQP1, AQP2, and NKCC2 mRNA levels tended to be higher in cyclophosphamide-treated rats than control rats, these changes were not statistically significant (Fig. 6).

In animal *experiment 2*, kidneys were harvested 72 h after single administration of a large dose (50 mg/kg BW) of cyclophosphamide (Fig. 1). Urine and plasma data from vehicle-treated controls ($n = 7$) and cyclophosphamide-treated rats ($n = 7$) revealed no significant differences (data not shown). Plasma levels of arginine vasopressin were not significantly different between vehicle-treated controls (*experiment 1*, 48.9 ± 4.1 pg/ml; *experiment 2*, 30.2 ± 10.6 pg/ml) and cyclophosphamide-administered rats (*experiment 1*, 58.1 ± 11.0 pg/ml; *experiment 2*, 54.3 ± 29.5 pg/ml). However, patterns of alterations in AQP2, NKCC2, and V2R expression in the kidney were consistent with those observed in animal *experiment 1*. As shown in Fig. 7, cyclophosphamide-treated rat kidneys were characterized by significant increases in expression of AQP1 (115 ± 4 vs. 100 ± 6%; $P < 0.05$), AQP2 (201 ± 26 vs. 100 ± 13%; $P < 0.01$), and NKCC2 (149 ± 12 vs. 100 ± 19%; $P < 0.05$) proteins vs. in vehicle-treated control kidneys. These immunoblot findings were confirmed by immunohistochemistry, as shown in Fig. 8. In qPCR analysis, both AQP2 (135 ± 5 vs. 100 ± 10%; $P < 0.05$) and V2R (127 ± 8 vs. 100 ± 9%; $P < 0.05$) mRNA levels were significantly increased above control levels by cyclophosphamide administration (Fig. 9).

Effects of 4-HC treatment on AQP2 and V2R expression in primary cultured IMCD cells. We tested whether the active cyclophosphamide metabolite 4-HC can directly regulate AQP2 and/or V2R expression in the absence of vasopressin. Immunoblot analysis of primary cultured IMCD cells revealed that treatment of these cells with a therapeutic concentration (10 μM) of 4-HC for 1 day induced an increase in AQP2

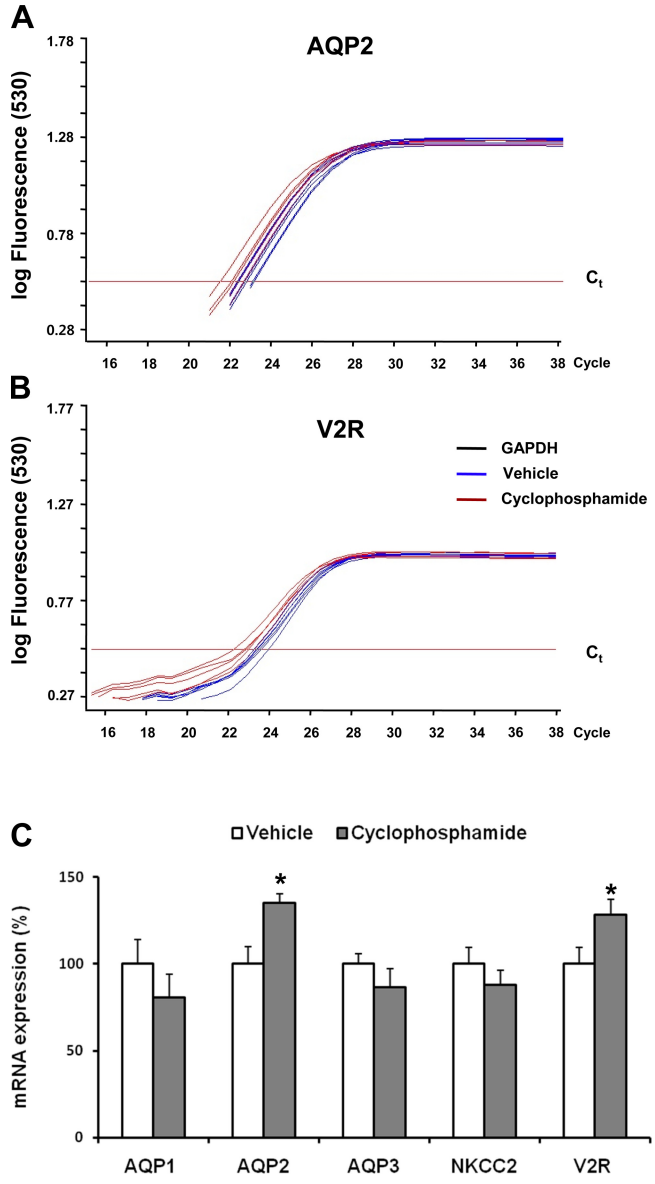

Fig. 9. Real-time quantitative PCR for AQP1, AQP2, AQP3, NKCC2, and V2R in rat kidneys from animal *experiment 2*. Kidneys were harvested 72 h after a single intraperitoneal administration of cyclophosphamide (50 mg/kg BW) in Sprague-Dawley rats. AQP2 (*A*) and V2R (*B*) graphs of fluorescence against cycle number were discriminated between vehicle-treated controls (blue) and cyclophosphamide-treated rats (red). Cyclophosphamide administration induced significant increases in AQP2 and V2R mRNA expression relative to control levels (*C*). Horizontal bar represents the C_t. *$P < 0.05$.

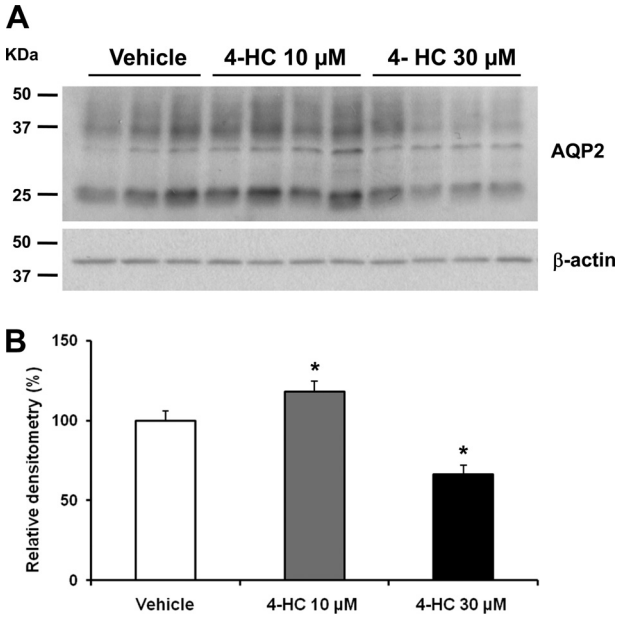

Fig. 10. *A*: immunoblots of AQP2 from primary cultured IMCD cells. Cells were treated with 2 different concentrations (10 and 30 μmol/l) of 4-hydroperoxycyclophosphamide (4-HC) for 24 h, and then immunoblotting was carried out. Each lane was loaded with a protein sample from a different Transwell filter support of IMCD cells. The immunoblots were reacted with anti-AQP2 (~29-kDa nonglycosylated and ~33- to 50-kDa glycosylated bands) and anti-β-actin antibody (~42 kDa). *B*: densitometric analyses showed that AQP2 protein abundance was increased by a lower dose of 4-HC (10 μmol/l, $n = 4$) but decreased by a higher dose (30 μmol/l, $n = 4$) of 4-HC compared with the vehicle ($n = 3$). *$P < 0.05$.

protein abundance (118 ± 8 vs. 100 ± 10%, $P < 0.05$), whereas a higher toxic concentration (30 μM) of 4-HC was associated with decreased AQP2 protein abundance (76 ± 12 vs. 100 ± 10%, $P < 0.05$, Fig. 10).

Laser-scanning confocal microscopy demonstrated that apical and lateral translocation of AQP2 was increased when IMCD cells were treated with 4-HC (10 μM) compared with vehicle-treated cells (*X-Z* images in Fig. 11, *A* and *B*). In contrast, intracellular labeling intensity of AQP2 decreased after 4-HC treatment (10 μM, Fig. 11, *A* and *B*). A toxic concentration of 4-HC (30 μM), however, was associated with markedly decreased AQP2 labeling intensity in the cells, and nuclei stained with DAPI were shrunken, possibly due to cell toxicity (Fig. 11*C*). To quantify 4-HC-induced subcellular redistribution of AQP2, pixel densities were measured as a function of apical-to-basal position. The *X-Z* images of AQP2-labeled IMCD cells were randomly selected, and the fluorescence intensities along the selected distance [60 pixels, from the apical pole (*position 0*) to the basal part (*position 60*) of the cells though the vertical lines drawn just next to the nuclei stained by DAPI in the cells] were acquired in each group. The results showed that, compared with vehicle-treated cells, both 4-HC (10 and 30 μM, 24 h) treatments induced a shift in AQP2 immunolabeling (490-nm excitation and 530-nm emission wavelengths) to the apical portion of the cells (Fig. 11, *D–G*).

To examine the changes in the mRNA levels of AQP2 and V2R in 4-HC-treated IMCD cells, qPCR was performed. Transcript levels of AQP2 (185 ± 27 vs. 100 ± 16%, $P < 0.05$) and V2R (221 ± 28 vs. 100 ± 4%, $P < 0.05$) were significantly higher in IMCD cells treated with 4-HC (10 μM) for 1 day than

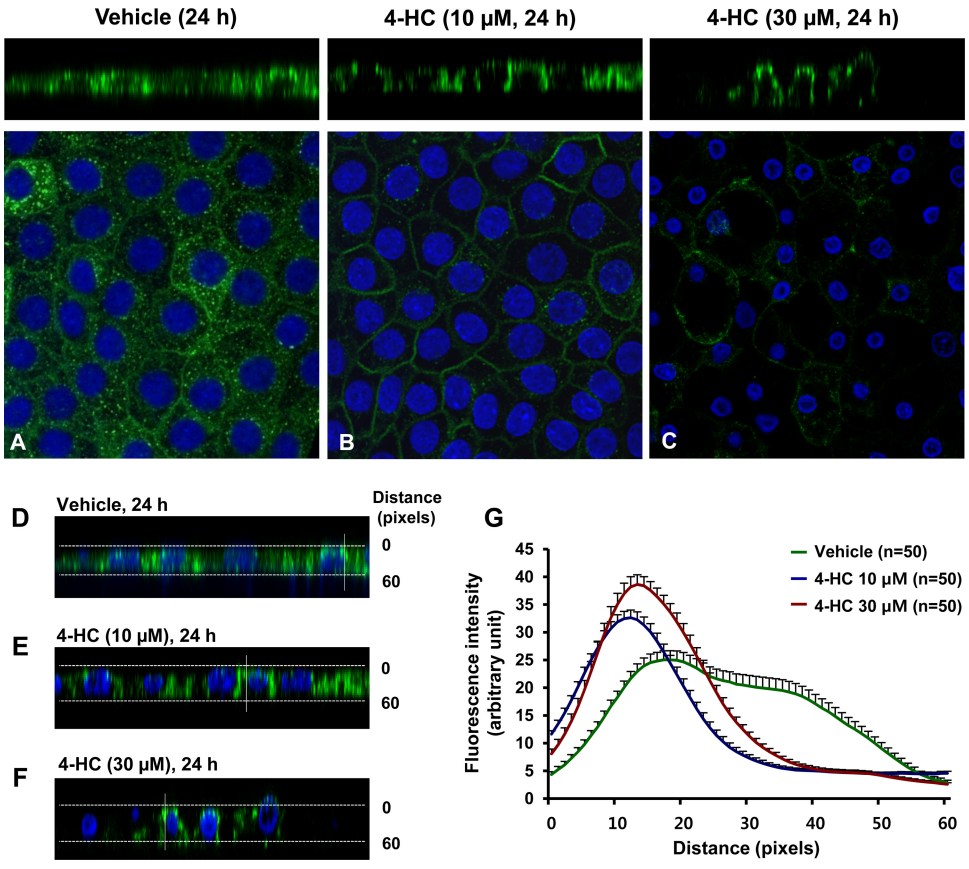

Fig. 11. Immunofluorescence microscopy of AQP2 in primary cultured IMCD cells. AQP2 labeling was localized mainly at the cytoplasm in the vehicle-treated control cells (*A*; *X-Z* image). In contrast, AQP2 targeting to the plasma membrane (apical and lateral translocation) was induced by treatment with 4-HC (10 and 30 μM) for 24 h (*B* and *C*; *X-Z* images). AQP2 immunolabeling intensity in the cytoplasm, however, was weaker in cells treated with 4-HC (*B* and *C*). Quantification of fluorescence intensity was used to demonstrate 4-HC-induced changes in the subcellular redistribution of AQP2 (*D–G*). The immunofluorescence intensities along the selected distance [60 pixels, from the apical pole (*position 0*) to the basal part (*position 60*) of the cells] though the vertical lines drawn just next to the nuclei stained by DAPI in the cells (white vertical lines in *D–F*) were measured in each group (*G*). The results showed that, compared with vehicle-treated cells, both 4-HC (10 and 30 μM, 24 h) treatments induced a shift in AQP2 immunolabeling to the apical pole of the cells (*D–G*). Four different Transwell filters per group were used for acquiring images, and the number (*n*) of the cells examined in each group was 50.

vehicle-treated cells. Graphs of SYBR green fluorescence from AQP2 and V2R as a function of number of cycles for control and experimental observations are presented in Fig. 12.

Effects of V2R antagonist cotreatment on 4-HC-induced AQP2 expression in primary cultured IMCD cells. To examine whether 4-HC-induced AQP2 expression was mediated by V2R stimulation, tolvaptan was cotreated in primary cultured IMCD cells. Immunoblotting of AQP2 was initially performed to evaluate the effects of tolvaptan cotreatment on dDAVP- or 4-HC-induced AQP2 expression and to determine the optimal dose of tolvaptan for inhibiting the effects of vasopressin stimulation on AQP2 expression (Fig. 13*A*). The results demonstrated that dDAVP (1 nM, basolateral, 24 h)-induced AQP2 expression was diminished by tolvaptan cotreatment (50 nM, basolateral, 27 h, Fig. 13*A*). This was also seen in 4-HC (10 μM)-treated IMCD cells, where 4-HC-induced AQP2 expression was attenuated by tolvaptan cotreatment (50 nM, basolateral, 27 h, Fig. 13*A*).

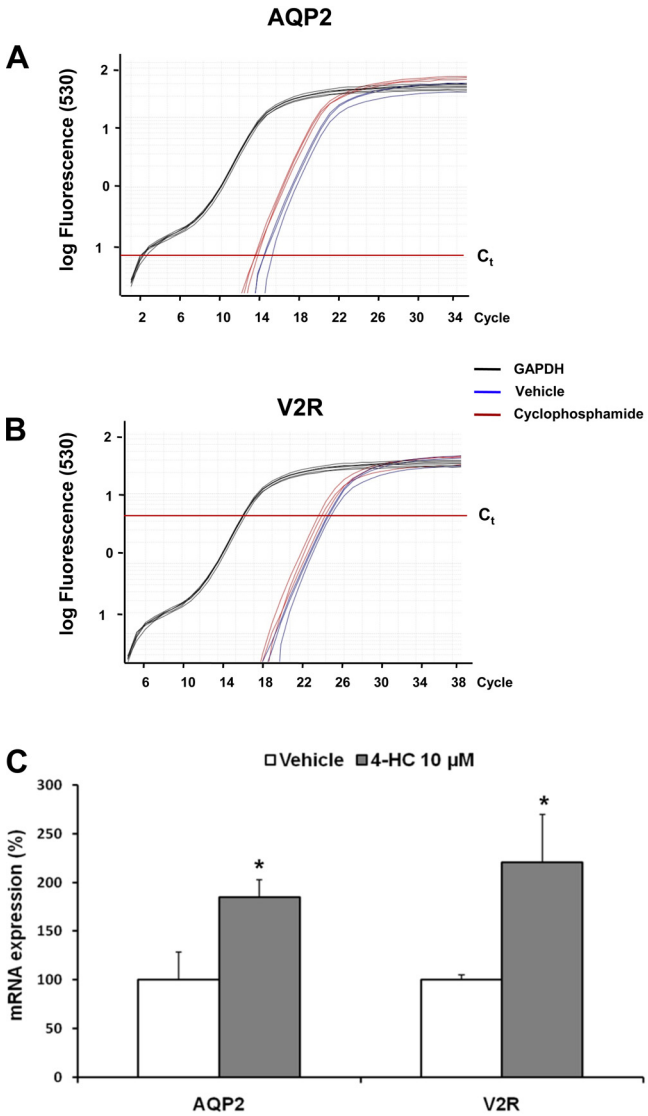

Fig. 12. Real-time quantitative PCR analysis of AQP2 and V2R levels in primary cultured IMCD cells. Cells were treated with vehicle ($n = 3$) and 4-HC (10 μM, $n = 3$) for 24 h. AQP2 (*A*) and V2R (*B*) graphs of fluorescence against cycle number were discriminated between vehicle-treated controls (blue) and cyclophosphamide-treated rats (red). Both AQP2 and V2R mRNA expression were significantly increased by 4-HC treatment relative to vehicle-only treatment (*C*). Quantitative real-time RT-PCR experiments for AQP2, V2R, and β-actin were performed 3 times independently. Horizontal bar represents the C_t. *$P < 0.05$.

Based on these results, 50 nM tolvaptan was used to evaluate whether 4-HC-induced AQP2 expression is blocked by a V2R antagonist. Figure 13, *B* and *C*, shows that AQP2 protein expression was significantly increased in 4-HC (10 μM)-treated cells (614 ± 149% of vehicle-treated control, $P < 0.05$) and that the 4-HC-induced increase in AQP2 expression was significantly attenuated when the cells were cotreated with tolvaptan (50 nM, basolateral, 27 h: 187 ± 22% of vehicle-treated control, $P < 0.05$ vs. 4-HC-treated cells, Fig. 13, *B* and *C*). The latter finding indicates that 4-HC may induce an increase in AQP2 protein via V2R stimulation.

Effects of V2R antagonist cotreatment on 4-HC-induced cAMP production in IMCD suspensions. To confirm the effects of tolvaptan cotreatment on 4-HC-induced upregulation of AQP2 and V2R in IMCD cells, we measured cAMP levels in response to 4-HC with and without tolvaptan cotreatment in rat IMCD suspensions. After incubation for 30 min, cAMP levels were significantly increased by 10 μM 4-HC (17.3 ± 0.6 pmol/mg protein) compared with vehicle-treated controls (8.5 ± 0.6 pmol/mg protein; $P < 0.01$). The 4-HC-induced increase in cAMP was comparable to that of 10 nM dDAVP treatment (20.5 ± 1.3 pmol/mg protein). Notably, it was significantly reduced by cotreatment with 100 nM tolvaptan (12.4 ± 1.1 pmol/mg protein, $P < 0.01$, Fig. 14).

DISCUSSION

The antidiuretic hormone (AVP)-V2R-cAMP-AQP2 water channel axis is so crucial that dysregulation of AVP-induced AQP2 is implicated in many clinical disorders of water homeostasis (21). In this study, we demonstrated that cyclophosphamide induces short-term upregulation of V2R and AQP2 expression in the kidney. Importantly, these results were confirmed in vitro in the absence of vasopressin stimulation. This novel finding may underlie the renal water retention induced by intravenous cyclophosphamide administration during management of rheumatological and malignant disorders.

Secretion of the antidiuretic hormone AVP is enhanced in most settings of hyponatremia. Impaired urinary dilution leading to water retention and hyponatremia is predominantly derived from nonosmotic stimulation of vasopressin release with upregulation of V2R and AQP2 expression (12, 33, 37). However, previous studies have shown that plasma vasopressin levels are not elevated in patients receiving various doses of cyclophosphamide (2, 5, 22). We also found no differences in plasma AVP between vehicle- and cyclophosphamide-treated animals. Thus cyclophosphamide-induced hyponatremia does not correspond to SIADH.

The term "syndrome of inappropriate antidiuresis (SIAD)" was proposed as an alternative to SIADH because a subgroup of patients with features of SIADH does not have elevated plasma vasopressin levels (32). Thus dilutional hyponatremia may be produced either by excessive AVP release (central) or by constitutive activation of V2R (nephrogenic). The latter type of SIAD is referred to as nephrogenic syndrome of inappropriate antidiuresis (NSIAD), and was originally de-

scribed from gain-of-function mutations of the V2 vasopressin receptor in two infants (16).

We also obtained results dissociating the upregulation of V2R from AVP release. In the absence of AVP stimulation, apical translocation of AQP2 was remarkably increased when primary cultured IMCD cells were treated with 4-HC, a major metabolite of cyclophosphamide. This effect was induced by a dose of 4-HC consistent with serum levels of toxic cyclophosphamide metabolites in patients that receive the prodrug (1, 8), although higher dosages produced cytotoxic effects. In addition, significant increases in AQP2 and V2R mRNA expression were demonstrated in both in vivo rat kidney and in vitro primary cultured IMCD cells. Moreover, AQP2 upregulation and cAMP accumulation in response to 4-HC were significantly reduced by tolvaptan cotreatment in primary cultured IMCD cells and IMCD suspensions, respectively. Thus, taken together, these results suggest the possibility of drug-induced NSIAD. A recent clinical study postulated NSIAD to be an underlying mechanism of hyponatremia in elderly patients treated with antidepressants (26). Interestingly, carbamazepine was reported to increase AQP2 expression in the rat IMCD (11). However, whether the expression of V2R is altered by drugs has not been explored.

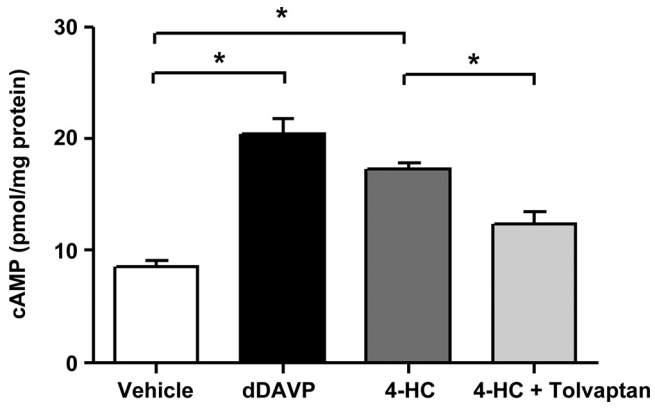

Fig. 14. Effects of V2R antagonist cotreatment on cAMP production in IMCD suspensions prepared from normal rat kidneys. IMCD suspensions were incubated with vehicle ($n = 5$), 10 nM 1-desamino-8-D-arginine vasopressin (dDAVP; $n = 8$), 10 μM 4-HC ($n = 8$), and 10 μM 4-HC+100 nM tolvaptan ($n = 8$) at 37°C for 30 min. Intracellular cAMP production was increased by 4-HC treatment and was significantly reduced by tolvaptan cotreatment. *$P < 0.05$.

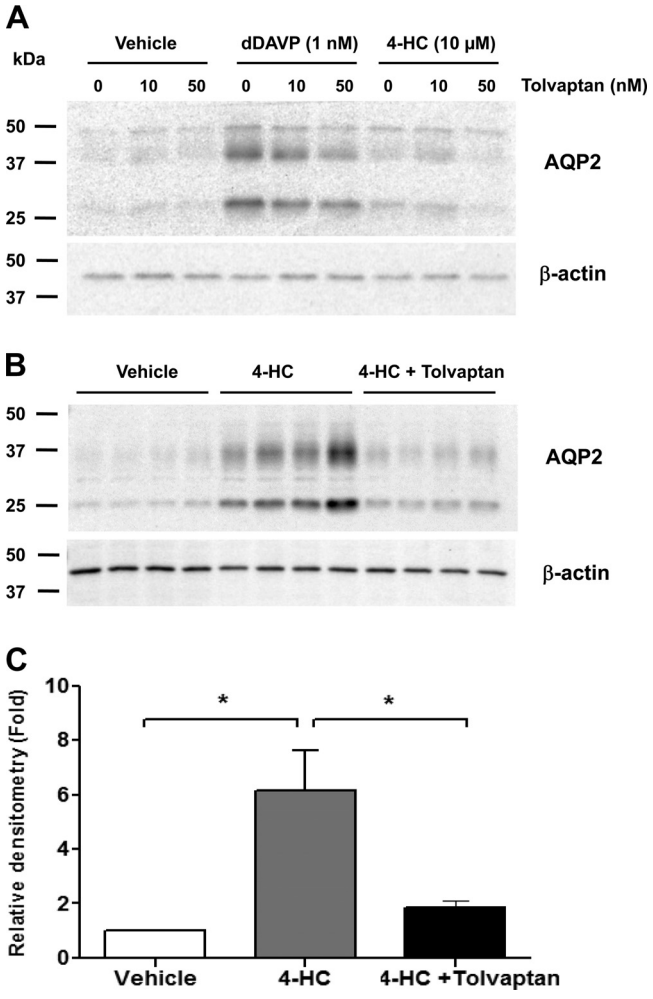

Fig. 13. Effects of V2R antagonist cotreatment on 4-HC-induced AQP2 protein expression in primary cultured IMCD cells. Immunoblot analysis of AQP2 was used to examine the effects of tolvaptan cotreatment (basolateral side only, pretreatment for 3 h+cotreatment for 24 h) on dDAVP (basolateral side only, 24 h) or 4-HC (basolateral side only, 24 h)-induced AQP2 expression (*A*) and to evaluate whether the 4-HC-induced AQP2 upregulation was blocked by the V2R antagonist cotreatment (*B*). AQP2 protein expression was significantly increased in 4-HC (10 μM)-treated cells compared with vehicle-treated controls (*B* and *C*; $n = 4$/group). The 4-HC-induced increase in AQP2 expression was significantly attenuated when cells were cotreated with tolvaptan (50 nM, basolateral, *B* and *C*; $n = 4$/group). *$P < 0.05$; n = number of preparations of IMCD cell lysates.

In this study, cyclophosphamide-induced upregulation of V2R was accompanied by increased expression of both AQP2 and NKCC2 in the apical membranes of the collecting duct and thick ascending limb, respectively. These results are consistent with the notion that V2R is located mainly in the collecting duct and thick ascending limb for the action of AVP (27). Increased expression of NKCC2 is likely to play an important role in enhancing the countercurrent multiplication system in the thick ascending limb (19) and would promote water retention from the collecting duct.

We also found that the expression of AQP1 was increased by cyclophosphamide, confirming our preliminary study findings (20). AQP1 is constitutively expressed in the apical and basolateral membranes of renal proximal tubules and descending thin limbs and does not participate in the regulation by vasopressin of renal water excretion (28). Thus its regulation remains elusive; our experiments showed that expression of AQP1 was altered by drug administration. Further studies are required to elucidate the intracellular pathways that regulate the expression of AQP1 in the renal proximal tubule. Few studies have investigated the regulation of AQP1, but angiotensin II may increase AQP1 expression in the kidney (4).

We conclude that in rat kidneys, cyclophosphamide may activate V2R and induce upregulation of AQP2 and NKCC2 or directly increase AQP2 trafficking in the absence of vasopressin stimulation. These intrarenal mechanisms suggest the possibility of drug-induced nephrogenic syndrome of inappropriate antidiuresis.

ACKNOWLEDGMENTS

We thank Dr. Wan Young Kim for technical assistance. We also appreciate the advice of Prof. Joong-Soo Han on this manuscript.

GRANTS

This study was supported by the Basic Science Research Program through the National Research Foundation of Korea (NRF) funded by the Ministry of Education, Science, and Technology (2010-0011799).

DISCLOSURES

No conflicts of interest, financial or otherwise, are declared by the authors.

AUTHOR CONTRIBUTIONS

Author contributions: S.K., H.-J.C., C.H.J., J.-S.P., and G.-H.K. performed experiments; S.K., H.-J.C., C.H.J., J.-S.P., T.-H.K., and G.-H.K. analyzed data; S.K., H.-J.C., C.H.J., J.-S.P., T.-H.K., and G.-H.K. interpreted results of experiments; S.K., H.-J.C., T.-H.K., and G.-H.K. prepared figures; S.K., T.-H.K., and G.-H.K. drafted manuscript; S.K., H.-J.C., C.H.J., J.-S.P., T.-H.K., and G.-H.K. approved final version of manuscript; J.-S.P., T.-H.K., and G.-H.K. edited and revised manuscript; G.-H.K. provided conception and design of research.

REFERENCES

1. **Anderson LW, Chen TL, Colvin OM, Grochow LB, Collins JM, Kennedy MJ, Strong JM.** Cyclophosphamide and 4-hydroxycyclophosphamide/aldophosphamide kinetics in patients receiving high-dose cyclophosphamide chemotherapy. *Clin Cancer Res* 2: 1481–1487, 1996.
2. **Bode U, Seif SM, Levine AS.** Studies on the antidiuretic effect of cyclophosphamide: vasopressin release and sodium excretion. *Med Pediatr Oncol* 8: 295–303, 1980.
3. **Bodó E, Tobin DJ, Kamenisch Y, Bíró T, Berneburg M, Funk W, Paus R.** Dissecting the impact of chemotherapy on the human hair follicle: a pragmatic in vitro assay for studying the pathogenesis and potential management of hair follicle dystrophy. *Am J Pathol* 171: 1153–1167, 2007.
4. **Bouley R, Palomino Z, Tang SS, Nunes P, Kobori H, Lu HA, Shum WW, Sabolic I, Brown D, Ingelfinger JR, Jung FF.** Angiotensin II and hypertonicity modulate proximal tubular aquaporin 1 expression. *Am J Physiol Renal Physiol* 297: F1575–F1586, 2009.
5. **Bressler RB, Huston DP.** Water intoxication following moderate-dose intravenous cyclophosphamide. *Arch Intern Med* 145: 548–549, 1985.
6. **Campbell DM, Atkinson A, Gillis D, Sochett EB.** Cyclophosphamide and water retention: mechanism revisited. *J Pediatr Endocrinol Metab*13: 673– 675, 2000.
7. **Chang TT, Gulati SC, Chou TC, Vega R, Gandola L, Ibrahim SM, Yopp J, Colvin M, Clarkson BD.** Synergistic effect of 4-hydroperoxycyclophosphamide and etoposide on a human promyelocytic leukemia cell line (HL-60) demonstrated by computer analysis. *Cancer Res* 45: 2434–2439, 1985.
8. **Chen TL, Kennedy MJ, Anderson LW, Kiraly SB, Black KC, Colvin OM, Grochow LB.** Nonlinear pharmacokinetics of cyclophosphamide and 4-hydroxycyclophosphamide/aldophosphamide in patients with metastatic breast cancer receiving high-dose chemotherapy followed by autologous bone marrow transplantation. *Drug Metab Dispos* 25: 544–551, 1997.
9. **Choi HJ, Yoon YJ, Kwon YK, Lee YJ, Chae S, Hwang D, Hwang GS, Kwon TH.** Patterns of gene and metabolite define the effects of extracellular osmolality on kidney collecting duct. *J Proteome Res* 11: 3816–3828, 2012.
10. **Chou CL, Rapko SI, Knepper MA.** Phosphoinositide signaling in rat inner medullary collecting duct. *Am J Physiol Renal Physiol* 274: F564–F572, 1998.
11. **de Bragança AC, Moyses ZP, Magaldi AJ.** Carbamazepine can induce kidney water absorption by increasing aquaporin 2 expression. *Nephrol Dial Transplant* 25: 3840–3845, 2010.
12. **Decaux G, Vandergheynst F, Bouko Y, Parma J, Vassart G, Vilain C.** Nephrogenic syndrome of inappropriate antidiuresis in adults: high phenotypic variability in men and women from a large pedigree. *J Am Soc Nephrol* 18: 606–612, 2007.
13. **DeFronzo RA, Braine H, Colvin M, Davis PJ.** Water intoxication in man after cyclophosphamide therapy. Time course and relation to drug activation. *Ann Intern Med* 78: 861–869, 1973.
14. **Ecelbarger CA, Chou CL, Lee AJ, DiGiovanni SR, Verbalis JG, Knepper MA.** Escape from vasopressin-induced antidiuresis: role of vasopressin resistance of the collecting duct. *Am J Physiol Renal Physiol* 274: F1161–F1166, 1998.
15. **Ecelbarger CA, Knepper MA, Verbalis JG.** Increased abundance of distal sodium transporters in rat kidney during vasopressin escape. *J Am Soc Nephrol* 12: 207–217, 2001.
16. **Feldman BJ, Rosenthal SM, Vargas GA, Fenwick RG, Huang EA, Matsuda-Abedini M, Lustig RH, Mathias RS, Portale AA, Miller WL, Gitelman SE.** Nephrogenic syndrome of inappropriate antidiuresis. *N Engl J Med* 352: 1884–1890, 2005.
17. **Hayashi M, Sasaki S, Tsuganezawa H, Monkawa T, Kitajima W, Konishi K, Fushimi K, Marumo F, Saruta T.** Role of vasopressin V2 receptor in acute regulation of aquaporin-2. *Kidney Blood Press Res* 19: 32–37, 1996.
18. **Jung HJ, Lim JS, Choi HJ, Lee MS, Kim JH, Kim SY, Kim S, Kim E, Kwon TH.** Vasopressin V2R-targeting peptide carrier mediates siRNA delivery into collecting duct cells. *PLoS One* 7: e40010, 2012.
19. **Kim GH, Ecelbarger CA, Mitchell C, Packer RK, Wade JB, Knepper MA.** Vasopressin increases Na-K-2Cl cotransporter expression in thick ascending limb of Henle's loop. *Am J Physiol Renal Physiol* 276: F96–F103, 1999.
20. **Kim S, Jo CH, Park JS, Han HJ, Kim GH.** The role of proximal nephron in cyclophosphamide-induced water retention: preliminary data. *Electrolyte Blood Press* 9: 7–15, 2011.
21. **Kwon TH, Frokiaer J, Nielsen S.** Regulation of aquaporin-2 in the kidney: a molecular mechanism of body-water homeostasis. *Kidney Res Clin Pract* 32: 96–102, 2013.
22. **Larose P, Ong H, du Souich P.** The effect of cyclophosphamide on arginine vasopressin and the atrial natriuretic factor. *Biochem Biophys Res Commun* 143: 140–144, 1987.
23. **Lee YC, Park JS, Lee CH, Bae SC, Kim IS, Kang CM, Kim GH.** Hyponatraemia induced by low-dose intravenous pulse cyclophosphamide. *Nephrol Dial Transplant* 25: 1520–1524, 2010.
24. **Lee YJ, Song IK, Jang KJ, Nielsen J, Frøkiaer J, Nielsen S, Kwon TH.** Increased AQP2 targeting in primary cultured IMCD cells in response to angiotensin II through AT_1 receptor. *Am J Physiol Renal Physiol* 292: F340–F350, 2007.
25. **Livak KJ, Schmittgen TD.** Analysis of relative gene expression data using real-time quantitative PCR and the $2^{-\Delta\Delta CT}$ method. *Methods* 25: 402–408, 2001.
26. **Mannesse CK, Jansen PA, Van Marum RJ, Sival RC, Kok RM, Haffmans PM, Egberts TC.** Characteristics, prevalence, risk factors, and underlying mechanism of hyponatremia in elderly patients treated with antidepressants: a cross-sectional study. *Maturitas* 76: 357–363, 2013.
27. **Mutig K, Paliege A, Kahl T, Jöns T, Müller-Esterl W, Bachmann S.** Vasopressin V2 receptor expression along rat, mouse, and human renal epithelia with focus on TAL. *Am J Physiol Renal Physiol* 293: F1166–F1177, 2007.
28. **Nielsen S, Smith B, Christensen EI, Knepper MA, Agre P.** CHIP28 water channels are localized in constitutively water-permeable segments of the nephron. *J Cell Biol* 120: 371–383, 1993.
29. **Park JS, Jo CH, Kim S, Kim GH.** Acute and chronic effects of dietary sodium restriction on renal tubulointerstitial fibrosis in cisplatin-treated rats. *Nephrol Dial Transplant* 28: 592–602, 2013.
30. **Park JS, Kim S, Jo CH, Oh IH, Kim GH.** Effects of dietary salt restriction on renal progression and interstitial fibrosis in adriamycin nephrosis. *Kidney Blood Press Res* 39: 86–96, 2014.
31. **Pa˘unescu TG, Lu HA, Russo LM, Pastor-Soler NM, McKee M, McLaughlin MM, Bartlett BE, Breton S, Brown D.** Vasopressin induces apical expression of caveolin in rat kidney collecting duct principal cells. *Am J Physiol Renal Physiol* 305: F1783–F1795, 2013.
32. **Robertson GL.** Regulation of arginine vasopressin in the syndrome of inappropriate antidiuresis. *Am J Med* 119, *Suppl* 1: S36–S42, 2006.
33. **Schrier RW.** Vasopressin and aquaporin 2 in clinical disorders of water homeostasis. *Semin Nephrol* 28: 289–296, 2008.
34. **Schrier RW, Sharma S, Shchekochikhin D.** Hyponatraemia: more than just a marker of disease severity? *Nat Rev Nephrol* 9: 37–50, 2013.
35. **Steele TH, Serpick AA, Block JB.** Antidiuretic response to cyclophosphamide in man. *J Pharmacol Exp Ther* 185: 245–253, 1973.
36. **Teicher BA, Holden SA, Goff DA, Wright JE, Tretyakov O, Ayash LJ.** Antitumor efficacy and pharmacokinetic analysis of 4-hydroperoxycyclophosphamide compared with cyclophosphamide ± hepatic enzyme effectors. *Cancer Chemother Pharmacol* 38: 553–560, 1996.
37. **Verbalis JG, Adler S, Schrier RW, Berl T, Zhao Q, Czerwiec FS; Investigators SALT.** Efficacy and safety of oral tolvaptan therapy in patients with the syndrome of inappropriate antidiuretic hormone secretion. *Eur J Endocrinol* 164: 725–732, 2011.